

## High-Resolution X-ray Photoelectron Spectroscopic Studies of Alkylated Silicon(111) Surfaces

Lauren J. Webb,<sup>†</sup> E. Joseph Nemanick,<sup>†</sup> Julie S. Biteen,<sup>†</sup> David W. Knapp,<sup>†</sup>  
David J. Michalak,<sup>†</sup> Matthew C. Traub,<sup>†</sup> Ally S. Y. Chan,<sup>‡</sup> Bruce S. Brunschwig,<sup>†</sup> and  
Nathan S. Lewis<sup>\*,†</sup>

Division of Chemistry and Chemical Engineering, California Institute of Technology, 210 Noyes Laboratory, 127-72, Pasadena, California 91125, and Department of Physics and Astronomy and Laboratory for Surface Modification, Rutgers University, Piscataway, New Jersey 08854

Received: June 28, 2004; In Final Form: October 27, 2004

Hydrogen-terminated, chlorine-terminated, and alkyl-terminated crystalline Si(111) surfaces have been characterized using high-resolution, soft X-ray photoelectron spectroscopy from a synchrotron radiation source. The H-terminated Si(111) surface displayed a Si 2p<sub>3/2</sub> peak at a binding energy 0.15 eV higher than the bulk Si 2p<sub>3/2</sub> peak. The integrated area of this shifted peak corresponded to one equivalent monolayer, consistent with the assignment of this peak to surficial Si–H moieties. Chlorinated Si surfaces prepared by exposure of H-terminated Si to PCl<sub>5</sub> in chlorobenzene exhibited a Si 2p<sub>3/2</sub> peak at a binding energy of 0.83 eV above the bulk Si peak. This higher-binding-energy peak was assigned to Si–Cl species and had an integrated area corresponding to 0.99 of an equivalent monolayer on the Si(111) surface. Little dichloride and no trichloride Si 2p signals were detected on these surfaces. Silicon(111) surfaces alkylated with C<sub>n</sub>H<sub>2n+1</sub>– (*n* = 1 or 2) or C<sub>6</sub>H<sub>5</sub>CH<sub>2</sub>– groups were prepared by exposing the Cl-terminated Si surface to an alkylmagnesium halide reagent. Methyl-terminated Si(111) surfaces prepared in this fashion exhibited a Si 2p<sub>3/2</sub> signal at a binding energy of 0.34 eV above the bulk Si 2p<sub>3/2</sub> peak, with an area corresponding to 0.85 of a Si(111) monolayer. Ethyl- and C<sub>6</sub>H<sub>5</sub>CH<sub>2</sub>-terminated Si(111) surfaces showed no evidence of either residual Cl or oxidized Si and exhibited a Si 2p<sub>3/2</sub> peak ~0.20 eV higher in energy than the bulk Si 2p<sub>3/2</sub> peak. This feature had an integrated area of ~1 monolayer. This positively shifted Si 2p<sub>3/2</sub> peak is consistent with the presence of Si–C and Si–H surface functionalities on such surfaces. The SXPS data indicate that functionalization by the two-step chlorination/alkylation process proceeds cleanly to produce oxide-free Si surfaces terminated with the chosen alkyl group.

### I. Introduction

There is currently considerable interest in developing chemical protection strategies for Si surfaces that prevent extensive uncontrolled oxidation of Si while preserving the low charge-carrier recombination velocity observed on the H-terminated Si(111) surface.<sup>1</sup> One promising approach is the formation of a wet-chemically prepared alkyl overlayer on the Si(111) surface. To this end, H-terminated surfaces have been alkylated with alkylmagnesium reagents,<sup>2,3</sup> and halogenated surfaces have been alkylated with alkylmagnesium or alkyllithium reagents.<sup>4–10</sup> The H-terminated silicon surface has been immersed in a variety of terminal alkenes and then functionalized through photolytic<sup>8,11–14</sup> or chemical free-radical activation,<sup>15,16</sup> thermal activation,<sup>16–22</sup> hydrosilylation,<sup>23–27</sup> or transition-metal-catalyzed reduction.<sup>28</sup> Other alkylation strategies involve forming dangling Si surface bonds by scanning tunneling microscopy techniques and reacting these dangling bonds with alkylating reagents.<sup>29</sup> Several electrochemical functionalization methods have also been described.<sup>30–37</sup>

A two-step surface alkylation procedure involving chlorination of H-terminated Si(111) followed by alkylation with an alkylmagnesium halide reagent has been shown to passivate the

surface to prevent both chemical oxidation and charge-carrier recombination on crystalline Si(111) surfaces during exposure to ambient air for periods of up to several weeks.<sup>10</sup> Extensive chemical passivation has been demonstrated on surfaces alkylated with straight-chain alkyls having 1–8 carbons atoms,<sup>10,38</sup> with branched alkyls such as *i*-propyl and *tert*-butyl and even with bulky functional groups such as phenyl and benzyl.<sup>39</sup> The success of this surface modification technique at chemical and electrical passivation is especially interesting in view of a simple steric model of the alkylated surface. The internuclear distance between adjacent atop sites on the Si(111) crystal face is 3.8 Å,<sup>40</sup> implying that a methyl group, with a van der Waals diameter of 2.5 Å,<sup>33</sup> is small enough to fit on every surface Si atom and 100% surface coverage is possible. Indeed, the close-packed CH<sub>3</sub>–Si(111) surface has been very recently observed using scanning tunneling microscopy at 4 K in ultrahigh vacuum.<sup>41</sup> In contrast, the van der Waals diameter of a methylene group is approximately 4.5–5 Å,<sup>42,43</sup> so complete termination of Si atop sites on an unreconstructed Si(111) surface is not possible. Models of alkyl packing on the Si(111) surface have indicated that 50–55% surface coverage is the maximum obtainable for long straight-chain alkyl groups on the Si(111) surface.<sup>42</sup> Bulkier functional groups such as *tert*-butyl or benzyl impose even more severe packing limitations on the alkylated Si(111) surface. Elucidation of the chemical

\* To whom correspondence should be addressed. E-mail: nslewis@its.caltech.edu.

<sup>†</sup> California Institute of Technology.

<sup>‡</sup> Rutgers University.

structures of such surfaces is important to understand the mechanism by which a large variety of alkylated Si surfaces, including those functionalized with lengthy or bulky substituents, are resistant toward chemical oxidation of the Si and additionally show relatively low levels of electrically active defect sites.

In this work, we describe detailed characterization of Si(111) surfaces alkylated with  $C_nH_{2n+1}-$  ( $n = 1$  and  $2$ ) and  $C_6H_5-CH_2-$  groups using high-resolution, "soft" X-ray photoelectron spectroscopy (SXPS). In these experiments, the alkylated Si surface is illuminated with a high-intensity beam of soft X-ray photons, enabling measurement of Si 2p photoelectrons with high spectral resolution and with low escape depths, thereby providing enhanced surface sensitivity over what is typically achievable in laboratory-based XPS instruments. The surface sensitivity of SXPS was used to identify and quantify surface Si atoms bonded to Cl, H, C, and O and to investigate the chemical species present on the nonalkylated portions of the functionalized Si surfaces.

## II. Experimental Section

**A. Materials and Methods. 1. Materials.** Silicon(111) wafers polished on one side and having a thickness of  $525\ \mu\text{m}$  were obtained from Crystec (Wilmington, OH). These n-type samples were doped with P to a resistivity of  $2\text{--}8.5\ \Omega\ \text{cm}$ .

All solvents used in alkylation reactions were anhydrous, stored under  $N_2(g)$ , and used as received from Aldrich Chemical Corp. Solvents were only exposed to the atmosphere of a  $N_2$ -(g)-purged flush box. Water with a resistivity of  $>17.8\ \text{M}\Omega\ \text{cm}$  obtained from a Barnstead Nanopure system was used at all times. All other chemicals were used as received.

**2. Sample Preparation.** Before chemical functionalization, each sample was cleaned by sequential immersion for 3 s each in a sonicated bath of  $CH_3OH$ , acetone,  $CH_2Cl_2$ , 1,1,1-trichloroethane (TCE),  $CH_2Cl_2$ , acetone, and  $CH_3OH$ . The sample was then rinsed with  $H_2O$ . Occasionally a different cleaning procedure was used, in which the sample was rinsed in flowing streams of  $H_2O$ ,  $CH_3OH$ , acetone,  $CH_3OH$ , and  $H_2O$ , respectively. After being cleaned, the sample was placed directly in 40%  $NH_4F(aq)$  (Transene, Inc.) for 20 min to etch the native oxide layer and produce a H-terminated Si(111) surface. During the etching process, the wafers were agitated occasionally to remove the bubbles that formed on the surface. After removal from the etching solution, the sample was rinsed thoroughly with  $H_2O$  and dried under a stream of  $N_2(g)$ . The sample was then either introduced into a quick-entry chamber of the ultra-high vacuum (UHV) system for XPS or SXPS analysis or placed into the antechamber of a  $N_2(g)$ -purged glovebox for further chemical functionalization.

Hydrogen-terminated Si(111) surfaces were chlorinated according to previously published procedures.<sup>4,10</sup> A freshly etched surface was first immersed in a saturated solution of  $PCl_5$  (99.998%, Alfa Aesar) in chlorobenzene to which a few grains of benzoyl peroxide had been added. The reaction solution was then heated to  $90\text{--}100\ ^\circ\text{C}$  for 45 min. The sample was then removed from the reaction solution, rinsed with tetrahydrofuran (THF),  $CH_3OH$ , and then THF, after which the THF was allowed to evaporate quickly from the sample surface. X-ray photoelectron spectra of the Cl-terminated surface were then collected.

For alkylation, the Cl-terminated Si(111) sample was immersed in a  $1.0\text{--}3.0\ \text{M}$  solution of  $C_nH_{2n+1}MgX$  in THF with  $n = 1$  or  $2$  and  $X = Cl$  or  $Br$  (Aldrich). Samples were also functionalized by immersion in a solution of  $2.0\ \text{M}$   $C_6H_5CH_2MgCl$  in THF (Aldrich). Excess THF was added to each reaction

solution to allow for solvent loss. The reaction solution was heated at  $70\text{--}80\ ^\circ\text{C}$  for  $3\text{--}4\ \text{h}$  for  $n = 1$ , for  $5\ \text{h}$  for  $n = 2$ , and for  $16\text{--}18\ \text{hr}$  for  $C_6H_5CH_2MgCl$ . At the end of the reaction, the sample was removed from the alkylmagnesium solution, rinsed with copious amounts of THF and  $CH_3OH$ , and then immersed in  $CH_3OH$  and removed from the  $N_2$ -purged glovebox. The sample was sonicated for 5 min in  $CH_3OH$ , sonicated in  $CH_3CN$  for a further 5 min, and then dried under a stream of  $N_2(g)$ . The alkyl-terminated sample was then introduced into the quick-entry load lock of the UHV chamber for core photoelectron spectroscopic analysis.

**B. Instrumentation. 1. XPS Measurements.** Preliminary spectroscopic data on functionalized Si(111) surfaces were collected using an M-Probe XPS system that has been described previously.<sup>4,10</sup> For these experiments,  $1486.6\ \text{eV}$  X-rays generated from an Al  $K\alpha$  source illuminated the sample from an incident angle of  $35^\circ$  off the surface. Photoelectrons emitted along a trajectory  $35^\circ$  off the surface were collected by a hemispherical analyzer. Samples were inserted via a quick-entry load lock into the UHV system and were kept at a base pressure of  $\leq 1 \times 10^{-9}$  Torr. All samples were sufficiently electrically conductive at room temperature that no compensation for charging effects was required. On each sample, a "survey" scan of core photoelectron binding energies from 1 to 1000 binding eV (BeV) was collected to identify the chemical species present on the surface.

A simple model that has been discussed previously<sup>44</sup> was used to determine the surface composition based on the relative intensities of the O 1s, C 1s, Cl 2s and 2p peaks, and Si 2p peaks observed in the survey XPS spectra. The equivalent monolayer coverage of an overlayer species,  $\Phi_{ov}$ , can be expressed as

$$\Phi_{ov} = \left[ \left( \frac{\lambda \sin \theta}{a_{ov}} \right) \left( \frac{SF_{Si}}{SF_{ov}} \right) \left( \frac{\rho_{Si}}{\rho_{ov}} \right) \left( \frac{I_{ov}}{I_{Si}} \right) \right] \quad (1)$$

where  $\lambda$  is the penetration depth (1.6 nm on this instrument);  $\theta$  is the photoelectron takeoff angle with respect to the surface ( $35^\circ$ );  $a_{ov}$  is the atomic diameter of the overlayer species; and  $\rho_x$  and  $I_x$  are the volumetric density and integrated area of the signal of the overlayer and Si, as indicated. The sensitivity factors ( $SF_x$ ) of the overlayer or substrate atoms used by the ESCA 2000 software package employed in this analysis were 0.90, 1.00, 2.49, 1.70, and 2.40 for the Si 2p, C 1s, O 1s, Cl 2s, and Cl 2p peaks, respectively. The solid-state volumetric densities ( $\rho_{ov}$ ) of C, O, and Cl (3, 0.92, and  $2.0\ \text{g cm}^{-3}$  respectively)<sup>44,45</sup> were used to calculate the atomic diameter of the overlayer species (0.19, 0.30, and 0.30 nm for C, O, and Cl, respectively) through the equation

$$a_{ov} = \left( \frac{A_{ov}}{\rho_{ov} N_A} \right)^{1/3} \quad (2)$$

where  $A_{ov}$  is the atomic weight of the overlayer species and  $N_A$  is Avogadro's number. The volumetric density of Si is  $\rho_{Si} = 2.328\ \text{g cm}^{-3}$ .<sup>40</sup> The integrated areas under the overlayer and substrate peaks,  $I_{ov}$  and  $I_{Si}$ , respectively, were determined by the ESCA 2000 software package.

**2. SXPS Measurements.** High-resolution SXPS experiments were performed on beamline U4A at the National Synchrotron Light Source (NSLS) at Brookhaven National Laboratory.<sup>46</sup> The sample was introduced through a quick-entry load lock into a two-stage UHV system that was maintained at pressures of  $\leq 1 \times 10^{-9}$  Torr. The beamline had a spherical grating monochro-

mator that selected photon energies between 10 and 200 eV with a resolution of 0.1 eV. The selected excitation energy was not calibrated independently because this study was principally concerned with shifts in the Si 2p binding energy in reference to the bulk Si 2p peak, as opposed to the determination of absolute binding energies. Samples were illuminated at an incident energy of 140 eV, and the emitted photoelectrons were collected normal to the sample surface by a VSW 100-mm hemispherical analyzer that was fixed at 45° off the axis of the photon source. The beam intensity from the synchrotron ring was measured independently, and the data in each scan were normalized to account for changes in photon flux during the scan. No charging or beam-induced damage was observed on the samples during data collection. The limited range of excitation energies available at this beamline, although well-suited for high-surface-resolution Si 2p core-level spectroscopy, precluded measurement of SXPS survey scans of the surface.

The escape depth of Si 2p photoelectrons was calculated using an empirical relation described by Seah.<sup>47</sup> The size of the Si atom,  $a_{\text{Si}}$ , was determined using eq 2 ( $A_{\text{Si}} = 28.086 \text{ g mol}^{-1}$  and  $\rho_{\text{Si}} = 2.328 \text{ g cm}^{-3}$ )<sup>40</sup> yielding  $a_{\text{Si}} = 0.272 \text{ nm}$ . The electron mean free path,  $\lambda_{\text{Si}}$ , was then calculated from the empirical relation<sup>47</sup>

$$\lambda_{\text{Si}} = (0.41 \text{ nm}^{-1/2} \text{ eV}^{-1/2}) a_{\text{Si}}^{1.5} E_{\text{Si}}^{0.5} \quad (3)$$

where  $E_{\text{Si}}$  is the electron kinetic energy (37 eV for Si 2p photoelectrons under our measurement conditions). Using this method,  $\lambda_{\text{Si}}$  of photoelectrons in the Si 2p peak was calculated to be 3.5 Å. Electron escape depths in Si measured under similar conditions have been reported to be 3.2–3.6 Å.<sup>48,49</sup> The penetration depth of the measurement can be calculated from  $l_{\text{Si}} = \lambda_{\text{Si}} \sin \theta$ , where  $\theta$  is the collection angle off the surface. Data presented here were collected at  $\theta = 90^\circ$ , so  $l_{\text{Si}} = 3.5 \text{ Å}$ .

To identify features in the Si 2p region in addition to the Si 2p bulk peak, the background was determined using a Shirley fitting procedure<sup>50–52</sup> and subtracted from the original spectra. The background-subtracted spectra were then processed to deconvolute, or “strip”, the Si 2p<sub>1/2</sub> peak from the spin–orbit doublet.<sup>49,53</sup> To perform the spin–orbit stripping procedure, the energy difference between the Si 2p<sub>3/2</sub> and Si 2p<sub>1/2</sub> peaks was fixed at 0.6 eV, and the Si 2p<sub>1/2</sub> to Si 2p<sub>3/2</sub> peak area ratio was fixed at 0.51.<sup>4,44,49,53</sup> The residual spectrum composed of Si 2p<sub>3/2</sub> peaks was then fitted to a series of Voigt line shapes<sup>54</sup> that were 5% Lorentzian and 95% Gaussian functions.<sup>10,44</sup> If more than one peak was needed to fit the spectrum, the full widths at half-maximum (fwhm) of all peaks were allowed to vary by  $\pm 25\%$  from each other.<sup>55</sup> Occasionally, results from the peak fitting procedure for a given spectrum would differ greatly with small changes in the initial conditions of the peak fit. To avoid bias in selecting a representative fit, multiple fits of the same data set, with different initial conditions, were averaged, and the average peak center and area, along with the standard deviation, are reported. This standard deviation represents a confidence level of the curve fitting procedure, as opposed to an estimate of random errors over multiple experimental measurements on nominally the same surface composition. Standard deviations obtained through this process were neglected if they were below the sensitivity of the instrument (0.01 eV, 0.02 monolayers).

A simple overlayer–substrate model was employed to calculate monolayer surface coverage. This model was independent of instrumental sensitivity factors, although it assumed negligible differences in the photoionization cross sections of surface and bulk Si species.<sup>10,44,53</sup> In this method, the number density of modified surface Si atoms,  $\Gamma_{\text{Si,surf}}$ , was deduced from

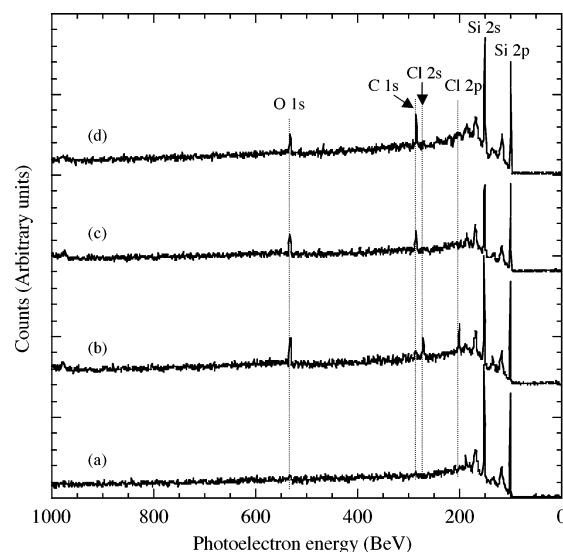


**Figure 1.** Survey X-ray photoelectron spectra of functionalized Si(111) surfaces prepared through a two-step chlorination/alkylation method: (a) H–Si(111), (b) Cl–Si(111), (c) CH<sub>3</sub>–Si(111), (d) C<sub>2</sub>H<sub>5</sub>–Si(111). Peak positions are given in the text.

the ratio of the integrated area under the Si peak assigned to the surface atoms,  $I_{\text{Si,surf}}$ , to the integrated area of the Si peak assigned to bulk Si atoms,  $I_{\text{Si,bulk}}$ , with

$$\frac{I_{\text{Si,surf}}}{I_{\text{Si,bulk}}} = \frac{\Gamma_{\text{Si,surf}}}{n_{\text{Si,bulk}} l_{\text{Si}} - \Gamma_{\text{Si,surf}}} \quad (4)$$

In this expression,  $n_{\text{Si,bulk}}$  is the number density of bulk crystalline Si atoms ( $5.0 \times 10^{22} \text{ cm}^{-3}$ ),<sup>40</sup> and  $l_{\text{Si}}$  is 3.5 Å. Substituting  $I = I_{\text{Si,surf}}/I_{\text{Si,bulk}}$  and  $\Gamma_{\text{Si,bulk}} = n_{\text{Si,bulk}} l_{\text{Si}}$  into eq 4 and rearranging yields

$$\Gamma_{\text{Si,surf}} = \frac{I}{1 + I} \Gamma_{\text{Si,bulk}} \quad (5)$$

Dividing the calculated value of  $\Gamma_{\text{Si,surf}}$  by the number density of atop sites on the Si(111) surface,  $7.8 \times 10^{14} \text{ cm}^{-2}$ ,<sup>53</sup> gives the monolayer coverage of modified Si atoms. The distance between Si layers along a vector perpendicular to the Si(111) crystal face is 1.6 Å,<sup>56</sup> implying that an electron escape depth of 3.5 Å will sample 2.2 monolayers of the Si crystal.

### III. Results

**A. H-Terminated Si(111) Surfaces.** Survey scan XPS data from a freshly etched H-terminated Si(111) surface exhibited peaks only for the Si 2p (99.9 BeV) and Si 2s (151.1 BeV) lines (Figure 1a). Peaks observed at successive intervals of 17.5 BeV higher than the two principal peaks are characteristic of crystalline silicon samples and have been identified previously as plasmon loss features that arise from the Si 2s and 2p photoelectrons.<sup>57,58</sup> The lack of C and O signals indicated that these elements were not present above the detection limit of the instrument, which was  $\sim 0.3$  monolayer for C and 0.2 monolayer for O.

Figure 2a shows the high-resolution SXPS data of the Si 2p region of a freshly prepared H-terminated Si(111) sample. As expected, a spin–orbit doublet was observed for bulk Si. As seen in the inset of Figure 2a, no silicon oxide signals were detected in the binding energy region up to 5 eV above the bulk peak, even under these surface-sensitive conditions.



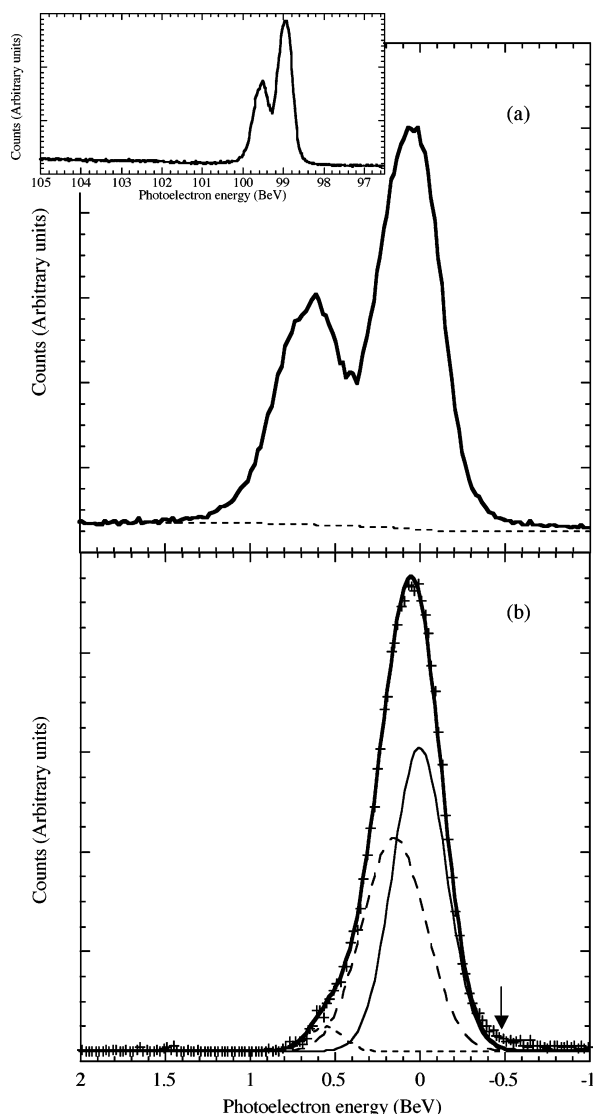


**Figure 2.** (a) SXPS results for the Si 2p region of a freshly prepared H-Si(111) surface and calculated background displayed relative to the binding energy (BeV) of the bulk Si 2p<sub>3/2</sub> signal. The inset shows the entire energy region that was examined, displayed as a function of the absolute binding energy measured before any data processing. (b) Background-subtracted Si 2p<sub>3/2</sub> region curve-fit as described in the text. Crosses, raw data; thin solid line, center at 98.89 BeV; long dashes, center at 99.04 BeV; short dashes, center at 99.44 BeV; thick solid line, calculated curve fit. The arrow identifies a feature discussed in the text.

Figure 2b shows the SXPS data remaining after background subtraction and stripping of the Si 2p<sub>1/2</sub> component of the Si spin-orbit doublet signal. The stripped data were fitted to a series of three Voigt functions: the bulk Si 2p<sub>3/2</sub> peak, a peak shifted higher in core binding energy by 0.15 eV, and a small foot shifted 0.55 eV higher in binding energy (Figure 2b). The 0.15 eV shift is consistent with expectations for surface Si atoms bonded to H, which display photoelectrons 0.114–0.250 eV higher in binding energy than those of bulk Si.<sup>59–61</sup> The magnitude and direction of this shift is consistent with expectations because H (Pauling electronegativity  $\chi_p = 2.20$ ) is somewhat more electronegative than Si ( $\chi_p = 1.90$ ).<sup>62</sup> The small peak shifted 0.55 eV higher than the bulk Si 2p<sub>3/2</sub> is possibly due to surface bound –OH groups that might have formed during the short time the sample was exposed to water vapor in air (<5 min) when it was placed into the vacuum system

(vide infra); however, no further experiments were conducted to determine the identity of this peak.

The low-binding-energy tail of the Si 2p<sub>3/2</sub> region shown in Figure 2b displayed a small signal that was not explained by the peak-fitting procedure. This feature appeared consistently in the Si 2p<sub>3/2</sub> spectra of all of the functionalized surfaces reported here and has been observed occasionally in the literature on chemically modified Si surfaces.<sup>9,61,63,64</sup> Limited efforts have been undertaken to investigate the source of this signal on an unreconstructed Si surface, with suggestions that this peak results from Si defects.<sup>61</sup> The small size of this feature did not interfere with the surface chemical analysis that was the focus of our investigations.

Table 1 summarizes the peak positions and surface coverages deduced from the fitting of the high-resolution XP spectra. The absolute energies of the bulk Si 2p<sub>3/2</sub> peaks observed for these surfaces are reported in Table 1, but because neither the excitation energy nor the work function of the instrument was measured during the experiment, the absolute energy observed has little meaning and will not be discussed further. On the H-Si(111) surface the +0.15 BeV peak was found to represent 1.02 ML of coverage (eq 5). The peak shifted by a binding energy of +0.55 eV had a coverage of 0.11 ML, again calculated using eq 5.

**B. Cl-Terminated Si(111) Surfaces.** As shown in Figure 1(b), a survey XPS scan of the Cl-terminated surface exhibited the expected bulk Si 2s and 2p peaks; an O 1s peak at 531.2 BeV; and Cl 2p and 2s peaks at 199.5 and 270.3 BeV, respectively. Use of eq 1 produced a value of  $0.73 \pm 0.13$  or  $0.59 \pm 0.08$  ML for the Cl surface coverage depending on whether the Cl 2s or Cl 2p peak was used. The same method produced a value of  $1.4 \pm 0.6$  ML for the coverage of O. If this oxygen were present as silicon oxide, the Si 2p oxide peaks at 101–105 BeV in the high-resolution photoelectron spectrum should contain approximately 50% of the total Si 2p intensity, because the instrumental configuration used in this work probed only 2.2 monolayers of the sample. The SXPS data of the Si 2p region of the Cl-terminated surface displayed in the inset of Figure 3a, however, clearly indicated a lack of observable SiO<sub>2</sub>, consistent with the hypothesis that the O 1s signal observed on these surfaces was due to adsorbed adventitious oxygen as opposed to silicon oxide.

The SXPS peaks in the Si 2p region of the Cl-Si(111) surface, shown in Figure 3a, were very different from those of the H-terminated Si surface. After the background had been removed and the spectrum stripped of the Si 2p<sub>1/2</sub> peak, a second Si 2p<sub>3/2</sub> signal was observed at a binding energy +0.83 eV relative to the bulk Si 2p<sub>3/2</sub> peak (Figure 3b). This second peak was assigned to Si bound to Cl ( $\chi_p = 3.16$ ).<sup>62</sup> Chlorine-terminated Si(111) surfaces prepared using UHV techniques have been reported previously to display Si 2p binding energy XPS peak shifts of 0.7–0.9 eV,<sup>56,65–69</sup> in good agreement with our observations. The signal at +0.83 BeV from the bulk Si 2p<sub>3/2</sub> peak represented an equivalent coverage of 0.99 ML. A third peak, located at a binding energy 1.37 eV higher than the Si 2p<sub>3/2</sub> peak, was much smaller in amplitude, comprising 0.16 of a monolayer. This binding energy shift is consistent with expectations for a Si atom bonded to two Cl atoms, which should exhibit a chemical shift approximately twice that of a Si monochloride species.

**C. Alkyl-Terminated Si(111) Surfaces. 1. CH<sub>3</sub>-Terminated Si(111) Surfaces.** Figure 1c displays a survey XP spectrum of the CH<sub>3</sub>-terminated Si(111) surface. The absence of Cl 2p and 2s peaks clearly indicated that Cl disappeared after exposure to

**TABLE 1: Si 2p<sub>3/2</sub> SXPS Data on Functionalized Si Surfaces**

surface	bulk peak <sup>a</sup> binding energy (eV)	peak 2 shift (eV)	peak 3 shift (eV)	equivalent monolayer coverage (ML) (eq 5)		
				peak 2	peak 3	total
H-Si(111)	98.89	0.15	0.55	1.02	0.11	1.13
Cl-Si(111) <sup>b</sup>	98.67 ± 0.04	0.83 <sup>c</sup>	1.37 <sup>c</sup>	0.99 ± 0.04	0.16 <sup>c</sup>	1.14 ± 0.04
CH <sub>3</sub> -Si(111) <sup>d</sup>	98.17 ± 0.02	0.34 ± 0.01	—	0.85 ± 0.03	—	0.85 ± 0.03
C <sub>2</sub> H <sub>5</sub> -Si(111) <sup>d</sup>	98.20 ± 0.01	0.19	0.61 ± 0.03	1.02 ± 0.12	0.19 ± 0.01	1.21 ± 0.13
C <sub>6</sub> H <sub>5</sub> CH <sub>2</sub> -Si(111) <sup>d</sup>	98.23 ± 0.02	0.15 ± 0.02	0.57 ± 0.02	1.10 ± 0.25	0.39 ± 0.08	1.49 ± 0.33

<sup>a</sup> Absolute energies for the bulk Si 2p<sub>3/2</sub> peak are reported for completeness but are of limited use because the excitation energy was not calibrated. <sup>b</sup> Error reported is one standard deviation from multiple identically prepared surfaces. <sup>c</sup> Variability in peak-fitting results was below the detection limit of our instrumental technique and was not considered meaningful. <sup>d</sup> Reported standard deviations are from multiple fits of the raw data for the same surface and represent a confidence level in the curve-fitting procedure.

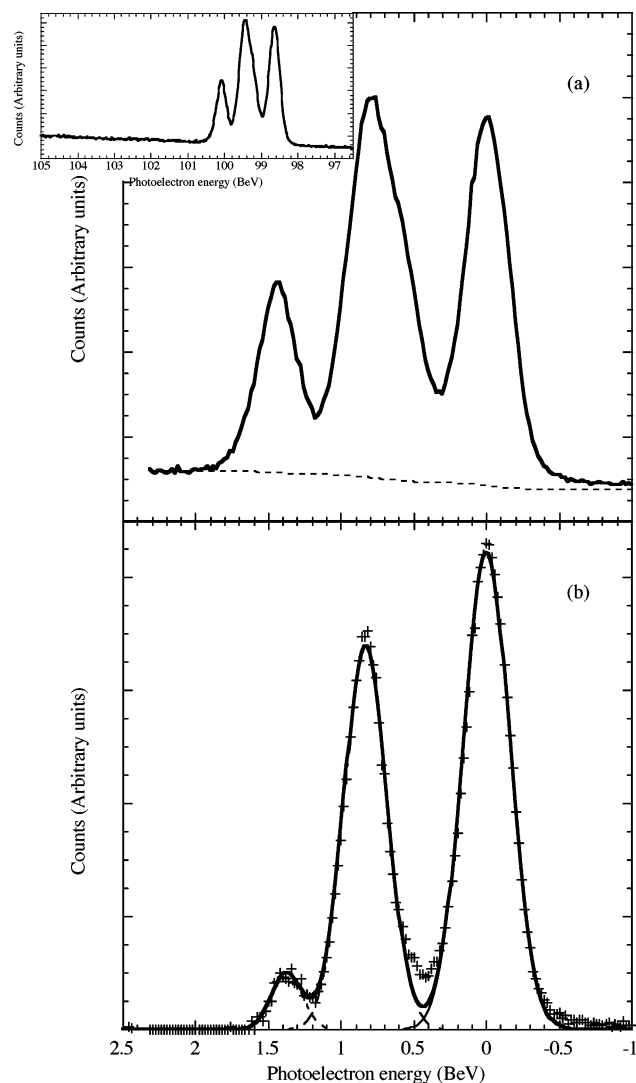


**Figure 3.** (a) SXPS results for the Si 2p region of a freshly prepared Cl-Si(111) surface and calculated background displayed relative to the binding energy (BeV) of the bulk Si 2p<sub>3/2</sub> signal. The inset shows the entire energy region that was examined, displayed as a function of the absolute binding energy measured before any data processing. (b) Background-subtracted Si 2p<sub>3/2</sub> region curve-fit as described in the text. Crosses, raw data; thin solid line, center at 98.64 BeV; long dashes, center at 99.47 BeV; short dashes, center at 100.01 BeV; thick solid line, calculated curve fit.

the methylmagnesium halide reagent, whereas a C 1s signal appeared at 284.7 BeV. An O 1s signal, ascribed to adventitious oxygen, was also visible on the functionalized surface at 531 BeV, representing  $1.27 \pm 0.01$  ML of surface monolayer coverage. As discussed above for the Cl-terminated surface, inspection of the core-level spectrum in the inset of Figure 4

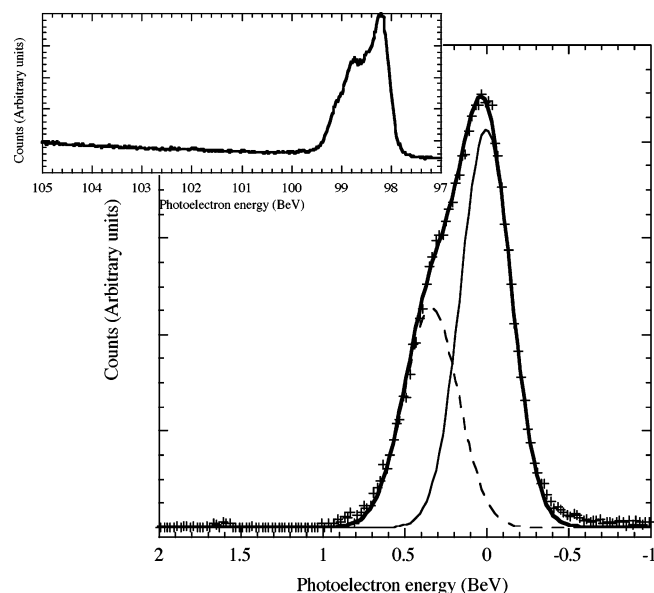


**Figure 4.** SXPS results for the Si 2p<sub>3/2</sub> region of a freshly prepared CH<sub>3</sub>-Si(111) surface after background subtraction and spin-orbit stripping. Crosses, raw data; thin solid line, center at 98.17 BeV; long dashes, center at 98.51 BeV; thick solid line, calculated curve fit. The inset shows the entire energy region that was examined, displayed as a function of the absolute binding energy measured before any data processing.

demonstrates that this O signal was not ascribable to oxidized silicon species.

Figure 4 shows the high-resolution SXPS data of the Si 2p region for a CH<sub>3</sub>-terminated Si(111) sample. A Si 2p<sub>3/2</sub> peak was observed 0.34 eV higher in binding energy than the bulk Si peak, consistent with expectations for a surface Si atom bonded to the more electronegative C ( $\chi_p = 2.55$ )<sup>62</sup> in the terminating methyl group. This second peak represented a coverage of 0.85 ML (Table 1). No signals were detected at binding energies greater than 1.0 eV relative to the bulk Si 2p<sub>3/2</sub> peak, indicating an absence of detectable oxidized silicon.

**2. C<sub>2</sub>H<sub>5</sub>-Terminated Si(111) Surfaces.** To determine the effect of alkylating the surface with groups that were sterically prevented from bonding to every Si atop site, the Si(111) surface was functionalized with a variety of straight-chain alkyls. The XPS wide-scan data on the C<sub>2</sub>H<sub>5</sub>-Si(111) surface (Figure 1d) resembled that of CH<sub>3</sub>-terminated Si(111) surface. This behavior was expected because the presence of adventitious hydrocarbon on the surface is known to complicate XPS analysis of terminating groups of similar C chain lengths.<sup>4</sup> The O 1s signal at 531 BeV ( $0.7 \pm 0.2$  ML) was ascribed to adventitious sources and not silicon oxides. High-resolution SXPS data from the Si 2p<sub>3/2</sub> peak on the freshly prepared C<sub>2</sub>H<sub>5</sub>-Si(111) surface, shown

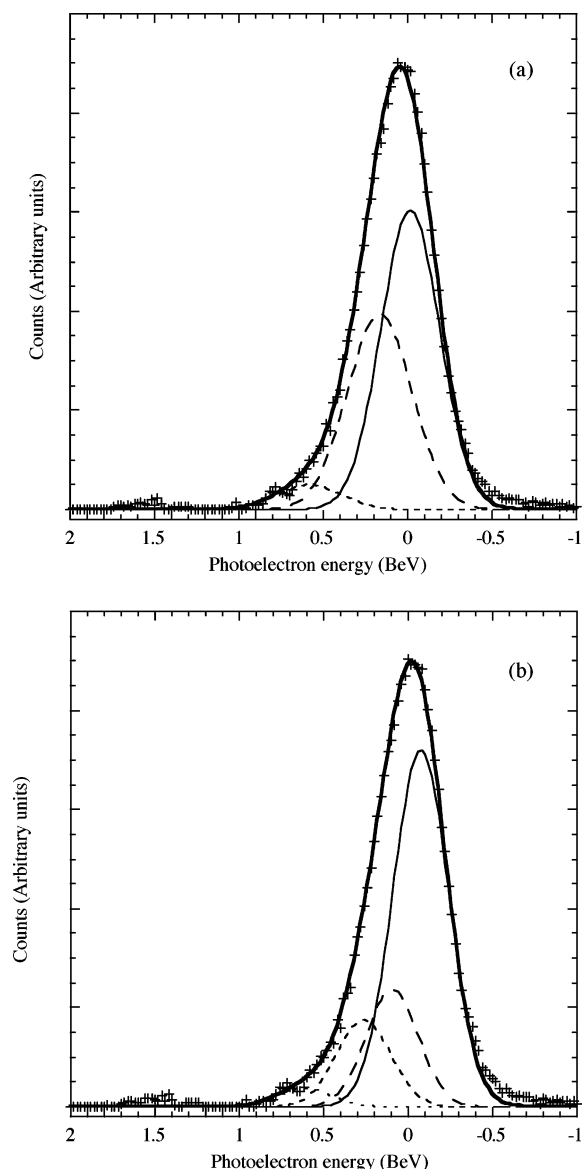


**Figure 5.** (a) SXPS results for the Si  $2p_{3/2}$  region of a freshly prepared  $C_6H_5CH_2$ -Si(111) surface after background subtraction and spin-orbit stripping. Crosses, raw data; thin solid line, center at 98.20 eV; long dashes, center at 98.39 eV; short dashes, center at 98.80 eV; thick solid line, calculated curve fit. (b) Same sample with the surface feature deconvoluted into two peaks representing Si-H (+0.18 eV) and Si-C (+0.34 eV).

in Figure 5a, exhibited a Si  $2p_{3/2}$  peak 0.19 eV higher in binding energy than the bulk Si  $2p_{3/2}$  peak. This shifted Si peak represented 1.02 ML of surface coverage. Similar to what was observed on the H-terminated surface, a third peak was present at 0.61 eV higher in energy than the bulk Si  $2p_{3/2}$  peak, in this case with a relative area corresponding to 0.19 of a monolayer. This peak possibly indicates a small oxygen-containing layer that could not be eliminated as the sample was introduced from air into the SXPS vacuum chamber. The total surface coverage of the two shifted peaks was 1.21 ML.

The peak +0.19 eV higher in energy than the bulk Si  $2p_{3/2}$  signal was approximately halfway between the peak energies for Si-H and Si-C signals observed on the H- and  $CH_3$ -terminated surfaces, respectively. To determine whether this peak resulted from two independent surface Si moieties, the peak was forced to be fitted by two peaks having the same energy shifts, shapes, and widths as those found on the H- and  $CH_3$ -Si surfaces. Although the fitting parameters were very

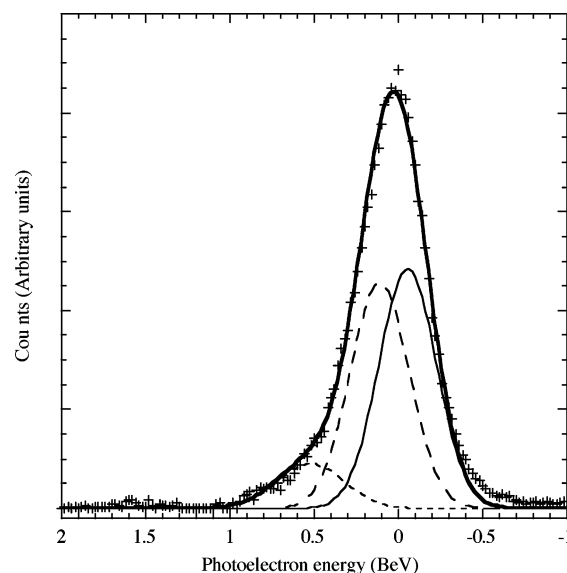


**Figure 6.** SXPS results for the Si  $2p_{3/2}$  region of a freshly prepared  $C_6H_5CH_2$ -Si(111) surface after background subtraction and spin-orbit stripping. Crosses, raw data; thin solid line, center at 98.22 BeV; long dashes, center at 98.39 BeV; short dashes, center at 98.80 BeV; thick solid line, calculated curve fit.

tightly constrained, there is a possibility that this procedure will result in overfitting of these spectral data. As shown in Figure 5b, this procedure produced a best fit with the two peaks at +0.18 and +0.34 eV representing coverages of 0.53 and 0.43 ML, respectively. A third peak, at +0.69 eV, representing a coverage of 0.11 ML was also present in the fit.

**3.  $C_6H_5CH_2$ -Terminated Si(111) Surfaces.** To investigate the effects of functionalization using longer and bulkier alkylating agents,  $C_6H_5CH_2$ -terminated Si(111) was prepared and studied by SXPS (Figure 6). As shown in Table 1, a Si  $2p_{3/2}$  peak was observed at 0.15 eV from the bulk peak with a coverage of 1.10 ML. A smaller peak 0.57 eV higher in binding energy than the bulk Si peak was also detected and was found to represent a coverage of approximately 0.39 ML. The coverage calculations are dependent on the calculated value of the electron escape depth, so a 0.2-Å increase in the calculated escape depth (to 3.7 Å) would produce a decrease in the calculated coverage of the two combined peaks to 1.2 ML.

#### IV. Discussion

Replacement of the H-terminated Si surface by a Si-Cl layer has been shown to yield a metastable intermediate surface that can be subsequently treated with an alkylmagnesium reagent, in an energetically favorable reaction, to drive the alkylation of Si to completion. The observed evolution of the high-resolution X-ray photoelectron spectra from the H- to Cl- to alkyl-terminated Si(111) surfaces clearly supported this formulation of the chemical transformations in the two-step chlorination/alkylation functionalization process. The H-terminated Si surface exhibited a distinct peak at +0.15 eV relative to the bulk Si  $2p_{3/2}$  peak, in accord with expectations for surficial Si-H bonds exhibiting a positive chemical shift due to the slightly increased electronegativity of H compared to Si. The determination that this surface has 1 monolayer coverage of such Si-H bonds is in agreement with other spectroscopically derived assignments of the structure of the  $NH_4F$ -etched Si(111) surface.<sup>70</sup>

Treatment with  $PCl_5$  eliminated the +0.15 eV Si  $2p_{3/2}$  peak observed on H-terminated Si(111) and produced peaks characteristic of a monochlorinated Si surface. The measured quantity



of surface Si–Cl groups was close to 1 ML, with peaks representing possible dichloro Si species accounting for <0.20 monolayer, and with no peaks attributable to trichloro Si species. Similar peak intensities and positions have been observed previously for H-terminated Si surfaces exposed to  $\text{Cl}_2(\text{g})$  under rigorously oxygen-free conditions.<sup>9</sup> Although XPS survey scans of the Cl-terminated sample showed some amount of O 1s signal, no  $\text{SiO}_2$  was detected between 101 and 105 BeV even under the highly surface sensitive conditions used here. The adventitious species could result from a number of sources, including adsorbed solvent from the wet-chemical preparation techniques, adsorbed pump oil vapor introduced in the quick-entry load lock, or contaminating dust particles covered with oxygen-containing organic molecules that were not possible to avoid when working in standard laboratory conditions. The Si 2p region, which has specific and extensively studied spectroscopic shifts introduced by  $\text{Si}^+ - \text{Si}^{4+}$  oxides<sup>49,53</sup> was examined instead to address this issue. The lack of oxidized silicon peaks demonstrates that the functionalization reaction proceeded without measurable Si oxidation under ambient pressure conditions in a  $\text{N}_2(\text{g})$  atmosphere.

The SXPS data also indicated that alkylation of the chlorinated Si surface proceeded without detectable silicon oxide formation. The lack of Cl signals on the methylated Si surfaces is consistent with the formation of a nearly full monolayer of Si– $\text{CH}_3$  bonds. The peak at +0.34 eV binding energy relative to the bulk Si  $2\text{p}_{3/2}$  peak is close to what has been observed previously for surficial Si atoms bonded to alkyl groups.<sup>9,71,72</sup> Previous SXPS studies of hydrocarbons introduced in UHV onto the Si(111)–( $7 \times 7$ ) surface have reported a Si  $2\text{p}_{3/2}$  peak shifted by  $\sim 0.5$  eV from the bulk Si  $2\text{p}_{3/2}$  peak, in accord with an expected shift of 0.4–0.5 eV based on simple electronegativity considerations.<sup>71,72</sup> Methylated Si surfaces prepared by treatment of a chlorinated Si(111) surface with  $\text{CH}_3\text{--Li}$  have also been reported to display Si  $2\text{p}_{3/2}$  SXPS peaks that are shifted by 0.27 eV from the bulk Si signal.<sup>9</sup> For the surfaces described here, the calculated coverage of the overlayer species was consistent with formation of nearly a full monolayer of Si– $\text{CH}_3$  groups. Furthermore, although some amount of adventitious O was again observed, the absence of peaks shifted by  $>1$  eV relative to bulk Si  $2\text{p}_{3/2}$  indicated that no silicon oxide with higher oxidation states was formed on the methylated surface.

Silicon(111) surfaces were further functionalized with longer, bulkier alkyl groups such as  $\text{C}_2\text{H}_5\text{--}$ , and  $\text{C}_6\text{H}_5\text{CH}_2\text{--}$ . Interestingly, no Si–Cl signals were detected on such surfaces, even when the alkyl group was precluded sterically from bonding to every Si atop site on an unreconstructed Si(111)–( $1 \times 1$ ) surface. Additionally, no oxide was detected on any alkylated surface. Contamination of the surface by Mg salts from the alkylmagnesium halide reagent was eliminated because no evidence for the Mg  $\text{K}_{1\text{L}_{23}}\text{L}_{23}$  Auger peak at 307 eV was observed in the XPS survey spectra of any alkylated surface (Figure 1d).

Because no elements other than Si, C, and O were detected in wide XPS scans of surfaces alkylated by the chlorination/alkylation procedure and because a negligible amount of oxidized Si was present on such alkylated surfaces, the unalkylated surface Si atoms are either reconstructed or have been terminated with Si–H bonds, presumably resulting from the quenching of the alkylmagnesium halide reagent with  $\text{CH}_3\text{--OH}$ . The Si–C binding energy shift is less than 0.2 eV greater than that of Si–H, making reliable decomposition of the two peaks difficult. However, the fittings to a single integrated peak and to two peaks at known Si–C and Si–H binding energy

shifts both were consistent with expectations for termination of a monolayer of Si atop atoms on such surfaces. Scanning probe microscopy studies and/or other independent spectroscopic signatures of such surfaces are required to assign the packing and fractional coverage of such systems by either Si–C or Si–H groups. These studies are ongoing in our laboratory.<sup>41</sup>

## V. Conclusions

High-resolution SXPS studies of crystalline Si(111) surfaces functionalized through a two-step wet-chemical route, involving chlorination of H–Si(111) followed by alkylation with a variety of alkylmagnesium reagents, have shown that on the H- or Cl-terminated Si(111) surface, a component of the Si 2p signal is shifted to higher binding energies than the bulk Si 2p peak, indicating a bonding interaction between a surface Si atom and an overlayer species that is more electronegative than the Si in the crystal lattice beneath the surface. Functionalization with  $\text{CH}_3$ , an alkyl group that can, in principle, bond to every atop site on the unreconstructed Si(111) surface, produced an SXPS signal in the Si  $2\text{p}_{3/2}$  region that was shifted to slightly higher energy than the bulk Si  $2\text{p}_{3/2}$  peak. The magnitude of this shift (+0.34 eV) is consistent with expectations for surface Si atoms bonded to the C atom of the methyl group. The intensity of this positively shifted signal corresponded to approximately 0.85 monolayer on the Si(111) surface. A similar (but lower-energy) peak was also observed on silicon surfaces that were functionalized with longer and bulkier functional groups that are sterically prohibited from forming bonds to every Si atop site on the Si(111) surface. The SXPS data indicate that such surfaces are partially alkyl-terminated and are either reconstructed or terminated at unalkylated sites with Si–H bonds. No evidence was found for Si–OR moieties or other oxidized Si species that could, in principle, contribute to the bonding of such surfaces. The detailed spectroscopic characterization of such functionalized surfaces is a required step in understanding the interesting chemical and electrical stability of these alkylated Si systems.

**Acknowledgment.** We gratefully acknowledge the National Science Foundation, Grant CHE-0213589, for support of this work and for providing a graduate research fellowship to L.J.W. A.C. acknowledges support from the Army Research Office. This research was carried out in part at the National Synchrotron Light Source, Brookhaven National Laboratory, which is supported by the U.S. Department of Energy, Division of Materials Sciences and Division of Chemical Sciences, under Contract DE-AC02-98CH10886. We thank Michael Sullivan for use of the  $\text{N}_2(\text{g})$ -purged glovebox at the NSLS.

## References and Notes

- (1) Yablonovitch, E.; Allara, D. L.; Chang, C. C.; Gmitter, T.; Bright, T. B. *Phys. Rev. Lett.* **1986**, *57*, 249–252.
- (2) Mitchell, S. A.; Boukherroub, R.; Anderson, S. J. *Phys. Chem. B* **2000**, *104*, 7668–7676.
- (3) Yu, H. Z.; Boukherroub, R.; Morin, S.; Wayner, D. D. M. *Electrochem. Commun.* **2000**, *2*, 562–566.
- (4) Bansal, A.; Li, X.; Yi, S. I.; Weinberg, W. H.; Lewis, N. S. *J. Phys. Chem. B* **2001**, *105*, 10266–10277.
- (5) Bansal, A.; Li, X. L.; Lauermann, I.; Lewis, N. S.; Yi, S. I.; Weinberg, W. H. *J. Am. Chem. Soc.* **1996**, *118*, 7225–7226.
- (6) He, J.; Patitsas, S. N.; Preston, K. F.; Wolkow, R. A.; Wayner, D. D. M. *Chem. Phys. Lett.* **1998**, *286*, 508–514.
- (7) Okubo, T.; Tsuchiya, H.; Sadakata, M.; Yasuda, T.; Tanaka, K. *Appl. Surf. Sci.* **2001**, *171*, 252–256.
- (8) Terry, J.; Linford, M. R.; Wigren, C.; Cao, R. Y.; Pianetta, P.; Chidsey, C. E. D. *Appl. Phys. Lett.* **1997**, *71*, 1056–1058.
- (9) Terry, J.; Linford, M. R.; Wigren, C.; Cao, R. Y.; Pianetta, P.; Chidsey, C. E. D. *J. Appl. Phys.* **1999**, *85*, 213–221.

- (10) Webb, L. J.; Lewis, N. S. *J. Phys. Chem. B* **2003**, *107*, 5404–5412.
- (11) Boukherroub, R.; Wayner, D. D. M. *J. Am. Chem. Soc.* **1999**, *121*, 11513–11515.
- (12) Cicero, R. L.; Linford, M. R.; Chidsey, C. E. D. *Langmuir* **2000**, *16*, 5688–5695.
- (13) Effenberger, F.; Gotz, G.; Bidlingmaier, B.; Wezstein, M. *Angew. Chem., Int. Ed.* **1998**, *37*, 2462–2464.
- (14) Terry, J.; Mo, R.; Wigren, C.; Cao, R. Y.; Mount, G.; Pianetta, P.; Linford, M. R.; Chidsey, C. E. D. *Nucl. Instrum. Methods Phys. Res. B* **1997**, *133*, 94–101.
- (15) Linford, M. R.; Chidsey, C. E. D. *J. Am. Chem. Soc.* **1993**, *115*, 12631–12632.
- (16) Linford, M. R.; Fenter, P.; Eisenberger, P. M.; Chidsey, C. E. D. *J. Am. Chem. Soc.* **1995**, *117*, 3145–3155.
- (17) Sieval, A. B.; Demirel, A. L.; Nissink, J. W. M.; Linford, M. R.; van der Maas, J. H.; de Jeu, W. H.; Zuilhof, H.; Sudholter, E. J. R. *Langmuir* **1998**, *14*, 1759–1768.
- (18) Sieval, A. B.; Linke, R.; Heij, G.; Meijer, G.; Zuilhof, H.; Sudholter, E. J. R. *Langmuir* **2001**, *17*, 7554–7559.
- (19) Sung, M. M.; Kluth, G. J.; Yauw, O. W.; Maboudian, R. *Langmuir* **1997**, *13*, 6164–6168.
- (20) Boukherroub, R.; Wojtyk, J. T. C.; Wayner, D. D. M.; Lockwood, D. J. *J. Electrochem. Soc.* **2002**, *149*, H59–H63.
- (21) Boukherroub, R.; Wayner, D. D. M.; Sproule, G. I.; Lockwood, D. J.; Canham, L. T. *Nano Lett.* **2001**, *1*, 713–717.
- (22) Boukherroub, R.; Wayner, D. D. M.; Lockwood, D. J.; Canham, L. T. *J. Electrochem. Soc.* **2001**, *148*, H91–H97.
- (23) Boukherroub, R.; Morin, S.; Bensebaa, F.; Wayner, D. D. M. *Langmuir* **1999**, *15*, 3831–3835.
- (24) Buriak, J. M.; Allen, M. J. *J. Am. Chem. Soc.* **1998**, *120*, 1339–1340.
- (25) Buriak, J. M.; Stewart, M. P.; Geders, T. W.; Allen, M. J.; Choi, H. C.; Smith, J.; Raftery, D.; Canham, L. T. *J. Am. Chem. Soc.* **1999**, *121*, 11491–11502.
- (26) Zazzera, L. A.; Evans, J. F.; Deruelle, M.; Tirrell, M.; Kessel, C. R.; McKeown, P. J. *Electrochem. Soc.* **1997**, *144*, 2184–2189.
- (27) Schmeltzer, J. M.; Porter, L. A.; Stewart, M. P.; Buriak, J. M. *Langmuir* **2002**, *18*, 2971–2974.
- (28) Saghatelian, A.; Buriak, J. M.; Lin, V. S. Y.; Ghadiri, M. R. *Tetrahedron* **2001**, *57*, 5131–5136.
- (29) Cicero, R. L.; Chidsey, C. E. D.; Lopinski, G. P.; Wayner, D. D. M.; Wolkow, R. A. *Langmuir* **2002**, *18*, 305–307.
- (30) Allongue, P.; de Villeneuve, C. H.; Pinson, J. *Electrochim. Acta* **2000**, *45*, 3241–3248.
- (31) Allongue, P.; de Villeneuve, C. H.; Pinson, J.; Ozanam, F.; Chazalviel, J. N.; Wallart, X. *Electrochim. Acta* **1998**, *43*, 2791–2798.
- (32) Dubois, T.; Ozanam, F.; Chazalviel, J.-N. *Electrochem. Soc. Proc.* **1997**, 97–7, 296–310.
- (33) Fidélis, A.; Ozanam, F.; Chazalviel, J. N. *Surf. Sci.* **2000**, *444*, L7–L10.
- (34) Gros-Jean, M.; Herino, R.; Chazalviel, J. N.; Ozanam, F.; Lincot, D. *Mater. Sci. Eng. B* **2000**, *69*, 77–80.
- (35) Henry de Villeneuve, C.; Pinson, J.; Bernard, M. C.; Allongue, P. *J. Phys. Chem. B* **1997**, *101*, 2415–2420.
- (36) Lees, I. N.; Lin, H. H.; Canaria, C. A.; Gurtner, C.; Sailor, M. J.; Miskelly, G. M. *Langmuir* **2003**, *19*, 9812–9817.
- (37) Allongue, P.; de Villeneuve, C. H.; Cherouvrier, G.; Cortes, R.; Bernard, M. C. *J. Electroanal. Chem.* **2003**, *550*, 161–174.
- (38) Royea, W. J.; Juang, A.; Lewis, N. S. *Appl. Phys. Lett.* **2000**, *77*, 1988–1990.
- (39) Nemanick, E. J.; Lewis, N. S., manuscript to be submitted.
- (40) Sze, S. M. *The Physics of Semiconductor Devices*, 2nd ed.; Wiley: New York, 1981.
- (41) Yu, H.; Webb, L. J.; Ries, R. S.; Solares, S. D.; Goddard, W. A.; Heath, J. R.; Lewis, N. S. *J. Phys. Chem. B* **2005**, *109*, 671–674.
- (42) Sieval, A. B.; van den Hout, B.; Zuilhof, H.; Sudholter, E. J. R. *Langmuir* **2001**, *17*, 2172–2181.
- (43) Ewen, B.; Strobl, G. R.; Richter, D. *Faraday Discuss.* **1980**, *69*, 19–31.
- (44) Haber, J. A.; Lewis, N. S. *J. Phys. Chem. B* **2002**, *106*, 3639–3656.
- (45) Greenwood, N. N.; Earnshaw, A. *Chemistry of the Elements*, 2nd ed.; Reed Educational and Professional Publishing Ltd.: Oxford, U.K., 1997.
- (46) Keister, J. W.; Rowe, J. E.; Kolodziej, J. J.; Niimi, H.; Tao, H. S.; Madey, T. E.; Lucovsky, G. *J. Vac. Sci. Technol. A* **1999**, *17*, 1250–1257.
- (47) Seah, M. P. Quantification of AES and XPS. In *Practical Surface Analysis*, 2nd ed.; Briggs, D., Seah, M. P., Eds.; John Wiley & Sons: Chichester, U.K., 1990; Vol. 1, pp 201–255.
- (48) Pi, T. W.; Hong, I. H.; Cheng, C. P.; Wertheim, G. K. *J. Electron Spectrosc. Relat. Phenom.* **2000**, *107*, 163–176.
- (49) Himpel, F. J.; Meyerson, B. S.; McFeeley, F. R.; Morar, J. F.; Taleb-Ibrahimi, A.; Yarmoff, J. A. Core Level Spectroscopy at Silicon Surfaces and Interfaces. In *Proceedings of the 1988 Enrico Fermi School on Photoemission and Absorption Spectroscopy of Solids and Interfaces with Synchrotron Radiation*; Varenna, North-Holland: Amsterdam, 1988; pp 203–236.
- (50) Proctor, A.; Sherwood, P. M. A. *Anal. Chem.* **1982**, *54*, 13–19.
- (51) Shirley, D. A. *Phys. Rev. B* **1972**, *5*, 4709–4714.
- (52) Contini, G.; Turchini, S. *Comput. Phys. Commun.* **1996**, *94*, 49–52.
- (53) Himpel, F. J.; McFeeley, F. R.; Taleb-Ibrahimi, A.; Yarmoff, J. A.; Hollinger, G. *Phys. Rev. B* **1988**, *38*, 6084–6096.
- (54) Sherwood, P. M. A. Data Analysis in XPS and AES. In *Practical Surface Analysis*; Briggs, D., Seah, M. P., Eds.; John Wiley & Sons Ltd.: New York, 1990; Vol. 1, pp 555–586.
- (55) Chakarian, V.; Shuh, D. K.; Yarmoff, J. A.; Hakansson, M. C.; Karlsson, U. O. *Surf. Sci.* **1993**, *296*, 383–392.
- (56) Durbin, T. D.; Simpson, W. C.; Chakarian, V.; Shuh, D. K.; Varekamp, P. R.; Lo, C. W.; Yarmoff, J. A. *Surf. Sci.* **1994**, *316*, 257–266.
- (57) Cheng, K. L.; Cheng, H. C.; Liu, C. C.; Lee, C.; Yew, T. R. *Jpn. J. Appl. Phys.* **1995**, *34*, 5527–5532.
- (58) Stinespring, C. D.; Wormhoudt, J. C. *J. Appl. Phys.* **1989**, *65*, 1733–1742.
- (59) Bjorkman, C. H.; Alay, J. L.; Nishimura, H.; Fukuda, M.; Yamazaki, T.; Hirose, M. *Appl. Phys. Lett.* **1995**, *67*, 2049–2051.
- (60) Blase, X.; Dasilva, A. J. R.; Zhu, X. J.; Louie, S. G. *Phys. Rev. B* **1994**, *50*, 8102–8105.
- (61) Karlsson, C. J.; Owman, F.; Landemark, E.; Chao, Y. C.; Martensson, P.; Uhrberg, R. I. G. *Phys. Rev. Lett.* **1994**, *72*, 4145–4148.
- (62) Allen, L. C. *J. Am. Chem. Soc.* **1989**, *111*, 9003–9014.
- (63) Hricovini, K.; Gunther, R.; Thiry, P.; Taleb-Ibrahimi, A.; Indlekofer, G.; Bonnet, J. E.; Dumas, P.; Petroff, Y.; Blase, X.; Zhu, X. J.; Louie, S. G.; Chabal, Y. J.; Thiry, P. A. *Phys. Rev. Lett.* **1993**, *70*, 1992–1995.
- (64) Ohishi, K.; Hattori, T. *Jpn. J. Appl. Phys.* **1994**, *33*, L675–L678.
- (65) Bogart, K. H. A.; Donnelly, V. M. *J. Appl. Phys.* **1999**, *86*, 1822–1833.
- (66) Layadi, N.; Donnelly, V. M.; Lee, J. T. C. *J. Appl. Phys.* **1997**, *81*, 6738–6748.
- (67) Cheng, C. C.; Guinn, K. V.; Donnelly, V. M.; Herman, I. P. *J. Vac. Sci. Technol. A: Vac. Surf. Films* **1994**, *12*, 2630–2640.
- (68) Yarmoff, J. A.; Shuh, D. K.; Durbin, T. D.; Lo, C. W.; Lapiano-smith, D. A.; McFeeley, F. R.; Himpel, F. J. *J. Vac. Sci. Technol. A: Vac. Surf. Films* **1992**, *10*, 2303–2307.
- (69) Schnell, R. D.; Rieger, D.; Bogen, A.; Himpel, F. J.; Wandelt, K.; Steinmann, W. *Phys. Rev. B* **1985**, *32*, 8057–8065.
- (70) Dumas, P.; Chabal, Y. J.; Higashi, G. S. *J. Electron Spectrosc. Relat. Phenom.* **1990**, *54*, 103–108.
- (71) Simons, J. K.; Frigo, S. P.; Taylor, J. W.; Rosenberg, R. A. *Surf. Sci.* **1996**, *346*, 21–30.
- (72) Rochet, F.; Jolly, F.; Bournel, F.; Dufour, G.; Sirotti, F.; Cantin, J. L. *Phys. Rev. B* **1998**, *58*, 11029–11042.